

# MicroRNA-145 plays a role in mitochondrial dysfunction in alveolar epithelial cells in lipopolysaccharide-induced acute respiratory distress syndrome

Yi Han, Su-cheng Mu, Jian-li Wang, Wei Wei, Ming Zhu, Shi-lin Du, Min Min, Yun-jie Xu, Zhen-ju Song, Chao-yang Tong

Emergency Department, Zhongshan Hospital, Fudan University, Shanghai 200032, China

**Corresponding Author:** Chao-yang Tong, Email: tong.chaoyang@zs-hospital.sh.cn; Zhen-ju Song, Email: song.zhenju@zs-hospital.sh.cn; Yun-jie Xu, Email: xu.yunjie@zs-hospital.sh.cn

**BACKGROUND:** Acute respiratory distress syndrome (ARDS) causes substantial mortalities. Alveolar epithelium is one of the main sites of cell injuries in ARDS. As an important kind of microRNAs (miRNAs), microRNA-145 (miR-145) has been studied in various diseases, while its role in ARDS has not been investigated.

**METHODS:** Lipopolysaccharide (LPS) was intratracheally instilled to establish a rat ARDS model. Cytokines from bronchoalveolar lavage fluid (BALF) were measured using rat tumor necrosis factor- $\alpha$  and interleukin-6 enzyme-linked immunosorbent assay kits (R&D Systems), and the pathological structures were evaluated using hematoxylin and eosin (H&E) staining and transmission electron microscope; the lung miR-145 messenger RNA (mRNA) was detected using quantitative polymerase chain reaction. Bioinformatics focused on the target genes and possible pathways of gene regulation.

**RESULTS:** A rat model of LPS-induced ARDS was successfully established. The miR-145 was down-regulated in the LPS-induced ARDS lung, and mitochondrial dysfunction was observed in alveolar epithelial cells, most obviously at 72 hours after LPS. TargetScan and miRDB databases were used to predict the target genes of miR-145. A total of 428 overlapping genes were identified, seven genes were associated with mitochondrial function, and *Ogt*, *Camk2d*, *Slc8a3*, and *Slc25a25* were verified. Kyoto Encyclopedia of Genes and Genomes (KEGG) pathways were enriched in the mitogen-activated protein kinase (MAPK) signaling pathway, and Gene Ontology (GO) biological process was mainly enriched in signal transduction and transcription regulation.

**CONCLUSIONS:** The miR-145 is down-regulated in LPS-induced ARDS, and affects its downstream genes targeting mitochondrial functions.

**KEYWORDS:** MicroRNA-145; Mitochondrial function; Lipopolysaccharide; Acute respiratory distress syndrome; Rats

World J Emerg Med 2021;12(1):54–60  
DOI: 10.5847/wjem.j.1920-8642.2021.01.009

## INTRODUCTION

Acute respiratory distress syndrome (ARDS) is a common condition associated with critical illnesses, which causes substantial mortalities. Approximately 200,000 ARDS cases per year occur in the USA, and the mortality is as high as 36%–44%.<sup>[1,2]</sup> Sepsis is often the main cause of ARDS, which may lead to multiple organ failure.<sup>[3]</sup> Lung inflammation, hypoxemia, and

non-cardiogenic pulmonary edema formation are characteristic features.<sup>[4,5]</sup>

Alveolar epithelium is one of the main sites of cell injuries in ARDS. Neutrophils contribute to lung inflammation and play important roles in the pathogenesis and progression of ARDS. The activated neutrophils damage epithelial cells,<sup>[6]</sup> which causes increased entry of fluid into the alveolar lumens,

decreased clearance of fluid from the alveolar airspace, and decreased production of surfactant.<sup>[7]</sup>

MicroRNAs (miRNAs) are small noncoding ribonucleic acid (RNA) molecules and are recognized as endogenous physiological regulators of gene expression.<sup>[8]</sup> Given that an individual miRNA could potentially alter complicated cellular processes including cell growth, apoptosis, inflammatory-immune responses, and cell-cell interaction,<sup>[9,10]</sup> it is not surprising that their wrong settings may be involved in the pathogenesis of ARDS.

Many miRNAs are expressed in the lung. MicroRNA-17 (miR-17), microRNA-92a (miR-92a), and microRNA-127 (miR-127) regulate the lung development.<sup>[11,12]</sup> Although miRNAs play a dominating role in several physiological functions, they are also involved in the pathogenesis of many diseases. The abnormal expression of miRNAs is associated with cardiac disorders,<sup>[13]</sup> vascular diseases,<sup>[14]</sup> cancers,<sup>[15]</sup> and pulmonary diseases like ARDS.<sup>[16]</sup>

As an important miRNA, microRNA-145 (miR-145) has been studied in various cancers.<sup>[15,17]</sup> It could potentially alter complex cellular processes, such as cell growth, cell cycle, apoptosis, and invasion.<sup>[18]</sup> A previous study reported that the expression of miR-145 was significantly reduced in myocardial ischemia/reperfusion (I/R) injury in the rats,<sup>[19]</sup> indicating that the abnormal expression of miR-145 was involved in myocardial I/R injury. Hypoxia could promote umbilical cord mesenchymal stem cell (UCMSC) differentiation into alveolar epithelial cells, and this effect was mainly mediated by miR-145.<sup>[20]</sup> Lipopolysaccharide (LPS)-induced liver inflammation was probably mediated by miR-145 through interleukin-1 receptor-associated kinase 1 (IRAK1) and nuclear factor-kappa B (NF- $\kappa$ B) pathways.<sup>[21]</sup> Furthermore, miR-145 suppression reversed the LPS-induced inflammatory injury on ATDC5 cells.<sup>[22]</sup>

However, the role of miR-145 in ARDS has not been investigated. In the present study, we aimed to identify miRNA-145 involved in ARDS by using an animal model of ARDS. In addition, we tried to focus on the relationship between miR-145 and mitochondrial function, which plays a critical role in regulating the cell injury of ARDS.

## METHODS

### Animals

The study was proved by the Ethics Department of Zhongshan Hospital, Fudan University. A total of 24 male Sprague-Dawley rats, aged 6–8 weeks, purchased from the Animal Center of Fudan University, and bred under pathogen free conditions, were housed separately

in a temperature-controlled room with a 12-hour light/12-hour dark cycle. Animals were allowed free access to food and water.

### Animal treatment

Rats were randomly assigned into two groups. They were anesthetized with an intraperitoneal injection of avertin (25 mg/kg) and fixed at a 60° angle on a table in a supine position. The oropharynx was lifted with forceps, allowing for the direct visualization of the trachea. LPS at a dose of 0.5 mg/kg (Sigma, USA) was injected into the trachea using an 18G catheter attached to a 1 mL syringe as previously described.<sup>[23]</sup> Control animals received an equal volume of phosphate-buffered saline (PBS). Rats were sacrificed at 6, 24, and 72 hours after LPS/PBS instillation after the intraperitoneal injection of avertin (25 mg/kg).

### RNA isolation and analysis

RNA was isolated from the median and caudal lobe of the right lung using the Qiagen RNeasy Mini Kit following the manufacturer's instructions. Quantitative polymerase chain reaction (qPCR) was performed for expressions of miRNAs using the primers for miR-145 as follows: 5'-GUCCAGUUUCCAGGAAUCCCU-3'.

### Determination of the lung water content

The right main bronchus was ligated, and the cranial and accessory lobes of the right lung were excised. After wet weights were measured, the cranial and accessory lobes of the right lung were placed in an oven at 60 °C for 72 hours to allow determination of the wet-to-dry (W/D) weight ratio.

### Bronchoalveolar lavage (BAL)

The BAL was performed in the left lung. Totally 2 mL PBS (4 °C) was slowly infused. The fluid was slowly withdrawn and reinfused for another two times. The recovered fluid was collected for further analysis.

### Cytokines in bronchoalveolar lavage fluid (BALF)

Tumor necrosis factor- $\alpha$  (TNF- $\alpha$ ) and interleukin-6 (IL-6) levels in BALF were measured using rat TNF- $\alpha$  and IL-6 enzyme-linked immunosorbent assay (ELISA) kits (R&D Systems) according to the manufacturer's recommendations.

### Hematoxylin and eosin (H&E) staining

Lung tissues were fixed and processed for H&E staining. Briefly, lung tissues were fixed by 10% PBS-buffered formalin through trachea catheterization at a

transpulmonary pressure of 15 cmH<sub>2</sub>O (1 cmH<sub>2</sub>O=0.098 kPa), and then overnight at 4 °C with agitation. After paraffin processing, the tissues were cut into semi-thin 4–5 μm thick and stained with H&E for histological analysis.

### Transmission electron microscope

The preparation of lung tissues for transmission electron microscopy was made following the procedure described previously.<sup>[24]</sup> Lung samples were obtained and fixed with 2.5% glutaraldehyde in PBS buffer. Then, lung samples were post-fixed with 1% OsO<sub>4</sub> in PBS buffer for 1 hour, followed by dehydration. Tissues were embedded in 50% propylene oxide/50% resin. Sectioning was performed on an ultramicrotome (60 nm thickness). Samples were stained with lead citrate, and examined with an electron microscope (Hitachi H-600, Japan).

### Target gene prediction of miRNA

The target genes of prognostic miR-145 were predicted using TargetScan and miRDB analysis tools. The overlapping genes were analyzed. Gene Ontology (GO) and Kyoto Encyclopedia of Genes and Genomes (KEGG) pathway enrichment analyses were performed for the target genes. The *P*-value <0.05 and gene count ≥3 were set as the cut-off criteria.

### Statistical analysis

The data were expressed as mean±standard deviation (SD). The expression levels of miRNAs in ARDS and control rats were analyzed by Wilcoxon signed-rank test. The *P*-value <0.05 was considered statistically significant. The statistical analysis was performed using SPSS software and Prism 6.0.

## RESULTS

### MiR-145 down-regulated in LPS-induced ARDS rat lung

With H&E staining, there were few inflammatory cells or lymphocyte infiltrations, and the structure of alveolar was almost intact in the control group; at 6 hours after LPS injection, the lymphocytes in the alveolar were significantly increased, especially increased around bronchi and lung vessels, and there was protein-like fluid filled in the alveola; at 24 hours after LPS injection, there were more lymphocyte infiltrations, the alveolar structures were disrupted and filled with inflammatory cells, and alveolar interval was much thicker than that in the control group; at 72 hours after LPS injection, the lymphocyte infiltrations still existed, but decreased compared with those at 24 hours (Figures

1A[a-d]). According to the lung injury scoring system,<sup>[25]</sup> scores significantly increased in LPS instillation lungs, especially at 24 hours and 72 hours after LPS injection (Figure 1B). At 6 hours after LPS injection, the W/D ratio of LPS lungs was about 7.5 compared with 3.0 in the control group; at 24 hours after LPS injection, the W/D ratio of LPS lungs was about 7.0, much higher than that in the control group (*P*<0.05); at 72 hours after LPS injection, the W/D ratio of LPS lungs was about 4.5, higher than that in the control group (*P*<0.05) (Figure 1C). The cytokines in BALF were measured at 6 hours (*n*=4), 24 hours (*n*=4), and 72 hours (*n*=4) after LPS instillation. The results showed that TNF-α peaked at 6 hours after LPS and gradually decreased; IL-6 peaked at 24 hours after LPS and gradually decreased to baseline at 72 hours (Figures 1D, E). The miR-145 messenger RNA (mRNA) expression was measured at 6, 24, and 72 hours after LPS instillation using qPCR. The results showed that with LPS instillation, the miR-145 expression was significantly decreased (Figure 1F).

### Mitochondrial dysfunction found in the epithelial cells of LPS-induced ARDS rat lung

The ultrastructure of alveolar epithelial cells was detected using a transmission electron microscope. There was a clear nuclear and lamellar bodies in the control lung epithelial cells, and the electron density of mitochondria was homogeneous. At 6 hours after LPS, the villi of epithelial cells turned incomplete, while there were still intact lamellar bodies and mitochondria. At 24 hours after LPS injection, the structures of the lamellar bodies and mitochondrial cristae were in disorder, and the electron density of mitochondria was gradually increased. At 72 hours after LPS injection, there was obvious structure disturbance of mitochondria and lamellar bodies, with the absence of mitochondrial cristae, which was the obvious evidence of mitochondrial injury (Figures 2A-D).

### Predicted target genes of miR-145 related to mitochondrial dysfunction

TargetScan and miRDB databases were used to search miR-145 so as to predict the target genes. A total of 428 overlapping genes were identified (Figure 3A). The enrichment analysis was performed to elucidate the biological function of target genes. The KEGG pathways were significantly enriched in mitogen-activated protein kinase (MAPK) signaling pathway and RAS signaling pathway. In addition, the GO biological process was mainly enriched in gene binding, signal transduction, and transcription regulation (Figures 3B,

C). Moreover, using the Rat Genome Database at the National Center for Biotechnology Information (NCBI), seven mitochondria-associated genes regulated by miR-145 were identified, including *Slc1a2*, *Cftr*, *Ogt*, *Acs14*, *Camk2d*, *Slc8a3*, and *Slc25a25*. All seven target genes were verified using qPCR in ARDS lungs. The results showed that *Ogt*, *Camk2d*, *Slc8a3*, and *Slc25a25* were slightly up-regulated at 24 hours after LPS injection, while significantly down-regulated at 72 hours after LPS injection ( $P<0.05$ ) (Figure 3D).

## DISCUSSION

ARDS is one of the most critical diseases in intensive care units (ICUs), which seriously affects the prognosis and life quality of critically ill patients. It is characterized by the acute onset of respiratory failure associated with diffuse interstitial pulmonary edema in the absence of left ventricular failure. It has been proved that the degeneration of surfactant is one of the most important causes of ARDS.

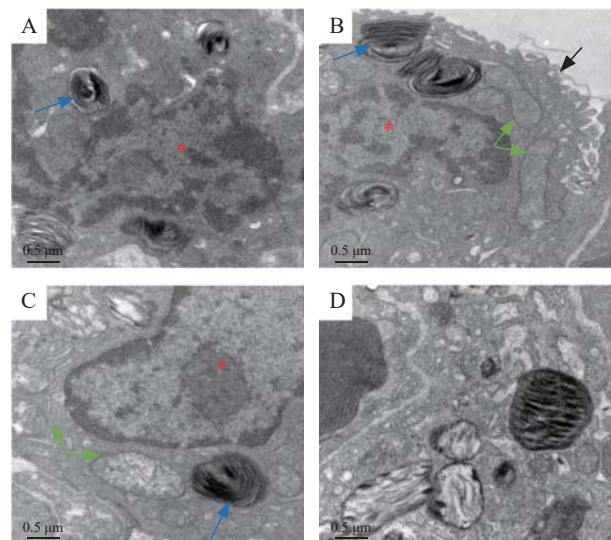


**Figure 2.** TEM structure of alveolar epithelial cell ( $\times 20,000$ ). Red star: nuclear of alveolar epithelial cell; blue arrow: lamellar bodies; green arrow: mitochondria; black arrow: villus of alveolar epithelial cell; A: control lung (72 hours after PBS); B: 6 hours after LPS instillation; C: 24 hours after LPS instillation; D: 72 hours after LPS instillation; TEM: transmission electron microscope; PBS: phosphate-buffered saline; LPS: lipopolysaccharide.

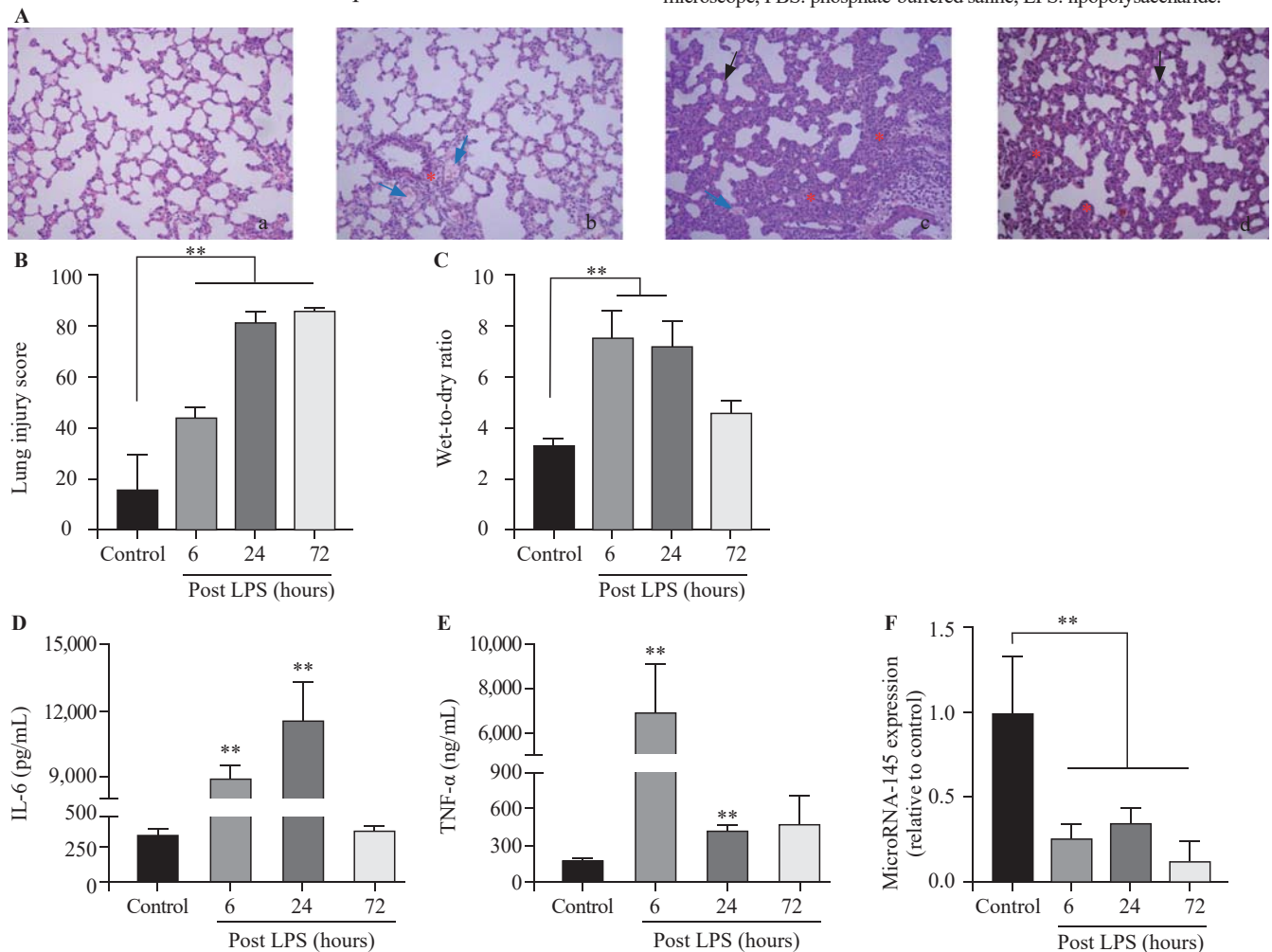


**Figure 1.** Rat lung microRNA-145 expression with LPS instillation. A: H&E staining,  $\times 10$ ; red star: lymphocytes infiltration; blue arrow: protein-like fluid filled in alveola; black arrow: alveolar interval thickened; a: control lung; b: 6 hours after LPS instillation; c: 24 hours after LPS instillation; d: 72 hours after LPS instillation; LPS: lipopolysaccharide; IL-6: interleukin-6; TNF- $\alpha$ : tumor necrosis factor- $\alpha$ ; \*\* $P<0.01$ .

Reduced secretion of surfactant is associated with worse outcome. A potential role for intact mitochondria in surfactant production and secretion is supported by studies reporting that intramitochondrial delivery of glutathione in rats significantly preserved surfactant producing and secreting functions of type II cells.<sup>[26]</sup>

LPS could induce inflammatory responses in various diseases, including ARDS.<sup>[21-23]</sup> The intratracheal instillation of LPS is proved to be an excellent *in vivo* model of lung injury, and it is widely used for

investigating ARDS. In our study, the results revealed that LPS up-regulated IL-6 and TNF- $\alpha$  expression, promptly stimulated cytokines responses, and significantly damaged the epithelial barrier. Inflammatory cells infiltrated in the alveolar air space and the para-vascular space, and the separation of alveola was much thickened after LPS instillation, which would finally form the hyaloid membrane in ARDS. With these pathological manifestations, we scored the inflammatory and structure disruption levels based on the previous

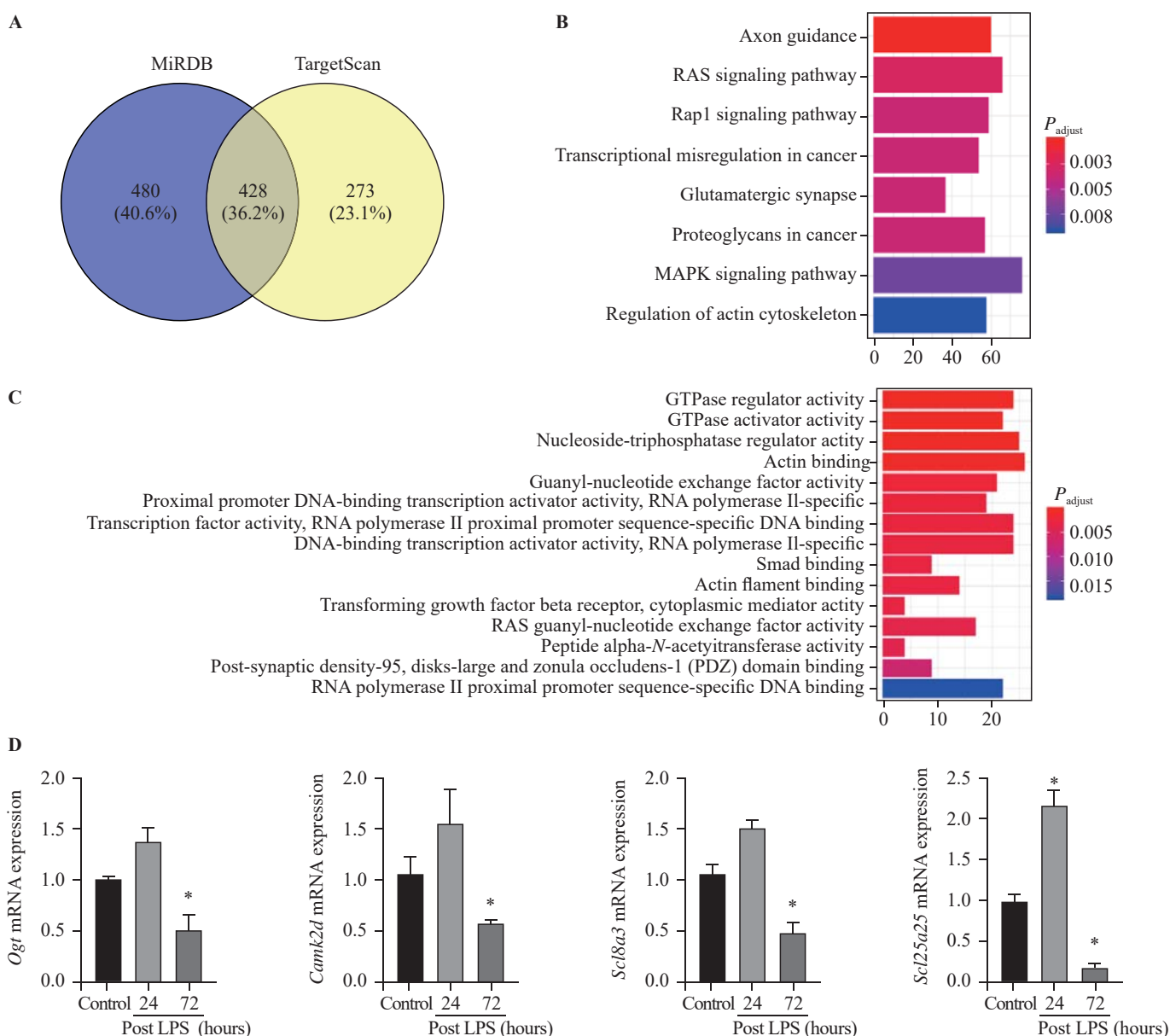


**Figure 3.** Bioinformatics data of microRNA-145 target genes and pathways. Compared with control, \* $P < 0.05$ ; A: target genes of microRNA-145 predicted using TargetScan and miRDB tools; B: KEGG pathway analysis (Y-axis representing the enriched KEGG terms, X-axis representing the amount of the microRNA-145-related mRNAs enriched in KEGG terms); C: GO biological process (Y-axis representing the enriched GO terms, X-axis representing the amount of the microRNA-145-related mRNAs enriched in GO terms); D: *Ogt*, *Camk2d*, *Scl8a3*, and *Scl25a25* mRNAs were slightly up-regulated at 24 hours post LPS instillation, while significantly down-regulated at 72 hours post LPS instillation; MAPK: mitogen-activated protein kinase; KEGG: Kyoto Encyclopedia of Genes and Genomes; GO: Gene Ontology; LPS: lipopolysaccharide.

study,<sup>[25]</sup> and we concluded that intratracheal instillation of LPS was a convenient and sufficient way to set up an ARDS model in rats.

The miRNAs are small non-coding RNAs that play a crucial role in many disease processes, including malignancy and inflammatory processes. Abnormal expression of miRNAs, such as miR-126-5p, miR-1246, miR-34a, miR-27a, and miR-223, has been found in lung injury.<sup>[23,27-30]</sup> MiR-145 is an important molecular marker, which has been proven to mediate cell proliferation, cell cycle, apoptosis, and invasion.<sup>[15]</sup> Researchers also found that miR-145 played a role in cervical epithelial cell barrier.<sup>[18]</sup> These studies demonstrated that miR-145 was associated with epithelial cell injury in cancer. However, whether miR-145 was involved in regulating LPS-induced ARDS remains unknown.

In our study, we found that the expression of miR-145 decreased in ARDS lungs, which was corresponding to the level of mitochondrial damage observed by transmission electron microscope (TEM) in lung epithelial cells. We found that the electron density of mitochondria began to increase at 24 hours after LPS injection, and there was obvious structure disturbance of mitochondria and lamellar bodies, as well as with the absence of mitochondrial cristae. As described in previous studies, miR-145 played an important role in regulating the mitochondrial apoptotic pathway in tumor cells, partly through its ability to target various anti-apoptotic molecules.<sup>[31]</sup> Moreover, the abnormal expression of miR-145 was associated with vascular smooth muscle cells' response to hydrogen peroxide-induced oxidative stress, indicating that miR-145 may participate in the regulation of the oxidative stress-triggered apoptosis and the regulation of the mitochondrial apoptotic pathway. Furthermore, programmed cell death 4 (PDCD4) was identified as a novel target of miR-145 in cardiomyocyte, and the overexpression of PDCD4 could remarkably restore the miR-145-inhibited cardiomyocyte apoptosis and mitochondrial dysfunction after hypoxia injury.<sup>[32]</sup> However, little is known about whether miR-145 is associated with lung epithelial cell apoptosis or how it interferes with the mitochondrial apoptotic pathway.

Previous studies have reported that inherited mitochondrial polymorphisms, genes, and pathways were associated with epithelial ovarian cancer risk, including TERF and PPARGC1a.<sup>[33]</sup> Cystic fibrosis transmembrane conductance regulator (CFTR) silencing results in lipid homeostasis disruption and mitochondrial dysfunction in intestinal epithelial cells, and it regulates neuronal apoptosis following cerebral I/R via mitochondrial oxidative stress-

dependent pathway.<sup>[34,35]</sup> *Ogt* is catalytically active *in vivo* and supports mitochondrial structure, health, and survival.<sup>[36]</sup> In our study, we found that *Ogt*, *Camk2d*, *Slc8a3*, and *Slc25a25* were significantly down-regulated at 72 hours after LPS injection, which verified the results that *Ogt*, *Camk2d*, *Slc8a3*, and *Slc25a25* were target genes of miR-145. Further studies are needed to confirm how miR-145 regulates its target genes, and to confirm the pathways we speculated from the bioinformatics data.

## CONCLUSIONS

The current study provided evidence related to the role of miR-145 in mitochondrial function in LPS-induced ARDS. The miR-145 was down-regulated in LPS-induced lung injury, which might affect its downstream genes targeting mitochondrial functions such as *Ogt*, *Camk2d*, *Slc8a3*, and *Slc25a25*. Bioinformatics data indicated that the regulation of miR-145 may be through MAPK and RAS signaling pathways. These results provide evidence that miR-145 may play a role in inflammatory-related epithelial barrier disruption, and further studies are needed to elucidate the specific mechanisms.

**Funding:** None.

**Ethical approval:** All applicable international, national, and institutional guidelines for the care and use of animals were followed. This article does not contain any studies with human participants.

**Conflicts of interests:** The authors declare that they have no competing interests.

**Contributors:** YH and SCM contributed equally to this work. CYT conceived the project, conducted the study, and gave administrative support to this study. SCM and JLW analyzed and interpreted the data. WW, MZ, and SLD contributed to data acquisition. MM helped with data analysis. ZJS and YJX revised the manuscript. CYT, ZJS, and YJX were co-corresponding authors. All authors read and approved the final manuscript.

## REFERENCES

- 1 Rubenfeld GD, Caldwell E, Peabody E, Weaver J, Martin DP, Neff M, et al. Incidence and outcomes of acute lung injury. *N Engl J Med*. 2005;353(16):1685-93.
- 2 Phua J, Badia JR, Adhikari NK, Friedrich JO, Fowler RA, Singh JM, et al. Has mortality from acute respiratory distress syndrome decreased over time?: A systematic review. *Am J Respir Crit Care Med*. 2009;179(3):220-7.
- 3 Thompson BT, Chambers RC, Liu KD. Acute respiratory distress syndrome. *N Engl J Med*. 2017;377(6):562-72.
- 4 Matthay MA, Zemans RL. The acute respiratory distress syndrome: pathogenesis and treatment. *Annu Rev Pathol*. 2011; 6:147-63.
- 5 Cepkova M, Matthay MA. Pharmacotherapy of acute lung injury

- and the acute respiratory distress syndrome. *J Intensive Care Med.* 2006;21(3):119-43.
- 6 Grommes J, Soehnlein O. Contribution of neutrophils to acute lung injury. *Mol Med.* 2011;17(3-4):293-307.
  - 7 Lowe K, Alvarez D, King J, Stevens T. Phenotypic heterogeneity in lung capillary and extra-alveolar endothelial cells. Increased extra-alveolar endothelial permeability is sufficient to decrease compliance. *J Surg Res.* 2007;143(1):70-7.
  - 8 Bartel DP. MicroRNAs: genomics, biogenesis, mechanism, and function. *Cell.* 2004;116(2):281-97.
  - 9 Hagen JW, Lai EC. MicroRNA control of cell-cell signaling during development and disease. *Cell Cycle.* 2008;7(15):2327-32.
  - 10 Chen CZ, Li L, Lodish HF, Bartel DP. MicroRNAs modulate hematopoietic lineage differentiation. *Science.* 2004;303(5654):83-6.
  - 11 Bhaskaran M, Wang Y, Zhang H, Weng T, Baviskar P, Guo Y, et al. MicroRNA-127 modulates fetal lung development. *Physiol Genomics.* 2009;37(3):268-78.
  - 12 Carraro G, El-Hashash A, Guidolin D, Tiozzo C, Turcatel G, Young BM, et al. MiR-17 family of microRNAs controls FGF10-mediated embryonic lung epithelial branching morphogenesis through MAPK14 and STAT3 regulation of E-Cadherin distribution. *Dev Biol.* 2009;333(2):238-50.
  - 13 Quiat D, Olson EN. MicroRNAs in cardiovascular disease: from pathogenesis to prevention and treatment. *J Clin Invest.* 2013;123(1):11-8.
  - 14 Zampetaki A, Mayr M. MicroRNAs in vascular and metabolic disease. *Circ Res.* 2012;110(3):508-22.
  - 15 Wang RK, Shao XM, Yang JP, Yan HL, Shao Y. MicroRNA-145 inhibits proliferation and promotes apoptosis of HepG2 cells by targeting ROCK1 through the ROCK1/NF- $\kappa$ B signaling pathway. *Eur Rev Med Pharmacol Sci.* 2019;23(7):2777-85.
  - 16 Cardinal-Fernández P, Ferruelo A, Esteban A, Lorente JA. Characteristics of microRNAs and their potential relevance for the diagnosis and therapy of the acute respiratory distress syndrome: from bench to bedside. *Transl Res.* 2016;169:102-11.
  - 17 Findlay VJ, Wang C, Nogueira LM, Hurst K, Quirk D, Ethier SP, et al. SNAI2 modulates colorectal cancer 5-fluorouracil sensitivity through miR145 repression. *Mol Cancer Ther.* 2014;13(11):2713-26.
  - 18 Anton L, DeVine A, Sierra LJ, Brown AG, Elovitz MA. MiR-143 and miR-145 disrupt the cervical epithelial barrier through dysregulation of cell adhesion, apoptosis and proliferation. *Sci Rep.* 2017;7(1):3020.
  - 19 Zhao ZH, Hao W, Meng QT, Du XB, Lei SQ, Xia ZY. Long non-coding RNA MALAT1 functions as a mediator in cardioprotective effects of fentanyl in myocardial ischemia-reperfusion injury. *Cell Biol Int.* 2017;41(1):62-70.
  - 20 Li Y, Shi X, Yang L, Mou Y, Li Y, Dang R, et al. Hypoxia promotes the skewed differentiation of umbilical cord mesenchymal stem cells toward type II alveolar epithelial cells by regulating microRNA-145. *Gene.* 2017;630:68-75.
  - 21 Xie R, Liu M, Li S. Emodin weakens liver inflammatory injury triggered by lipopolysaccharide through elevating microRNA-145 *in vitro* and *in vivo*. *Artif Cells Nanomed Biotechnol.* 2019;47(1):1877-87.
  - 22 Liu M, Zhang J, Liu W, Wang W. Salidroside protects ATDC5 cells against lipopolysaccharide-induced injury through up-regulation of microRNA-145 in osteoarthritis. *Int Immunopharmacol.* 2019;67:441-8.
  - 23 Ju M, Liu B, He H, Gu Z, Liu Y, Su Y, et al. MicroRNA-27a alleviates LPS-induced acute lung injury in mice via inhibiting inflammation and apoptosis through modulating TLR4/MyD88/NF- $\kappa$ B pathway. *Cell Cycle.* 2018;17(16):2001-18.
  - 24 Graham L, Orenstein JM. Processing tissue and cells for transmission electron microscopy in diagnostic pathology and research. *Nat Protoc.* 2007;2(10):2439-50.
  - 25 Matute-Bello G, Downey G, Moore BB, Groshong SD, Matthay MA, Slutsky AS, et al. An official American Thoracic Society workshop report: features and measurements of experimental acute lung injury in animals. *Am J Respir Cell Mol Biol.* 2011;44(5):725-38.
  - 26 Guidot DM, Brown LA. Mitochondrial glutathione replacement restores surfactant synthesis and secretion in alveolar epithelial cells of ethanol-fed rats. *Alcohol Clin Exp Res.* 2000;24(7):1070-6.
  - 27 Tang R, Pei L, Bai T, Wang J. Down-regulation of microRNA-126-5p contributes to overexpression of VEGFA in lipopolysaccharide-induced acute lung injury. *Biotechnol Lett.* 2016;38(8):1277-84.
  - 28 Shetty SK, Tiwari N, Marudamuthu AS, Puthusseri B, Bhandary YP, Fu J, et al. p53 and miR-34a feedback promotes lung epithelial injury and pulmonary fibrosis. *Am J Pathol.* 2017;187(5):1016-34.
  - 29 Neudecker V, Brodsky KS, Clambey ET, Schmidt EP, Packard TA, Davenport B, et al. Neutrophil transfer of miR-223 to lung epithelial cells dampens acute lung injury in mice. *Sci Transl Med.* 2017;9(408):eaah5360.
  - 30 Fang Y, Gao F, Hao J, Liu Z. MicroRNA-1246 mediates lipopolysaccharide-induced pulmonary endothelial cell apoptosis and acute lung injury by targeting angiotensin-converting enzyme 2. *Am J Transl Res.* 2017;9(3):1287-96.
  - 31 Zhou J, Gong J, Ding C, Chen G. Quercetin induces the apoptosis of human ovarian carcinoma cells by upregulating the expression of microRNA-145. *Mol Med Rep.* 2015;12(2):3127-31.
  - 32 Xu H, Cao H, Zhu G, Liu S, Li H. Overexpression of microRNA-145 protects against rat myocardial infarction through targeting PDCD4. *Am J Transl Res.* 2017;9(11):5003-11.
  - 33 Permutth-Wey J, Chen YA, Tsai YY, Chen Z, Qu X, Lancaster JM, et al. Inherited variants in mitochondrial biogenesis genes may influence epithelial ovarian cancer risk. *Cancer Epidemiol Biomarkers Prev.* 2011;20(6):1131-45.
  - 34 Zhang YP, Zhang Y, Xiao ZB, Zhang YB, Zhang J, Li ZQ, et al. CFTR prevents neuronal apoptosis following cerebral ischemia reperfusion via regulating mitochondrial oxidative stress. *J Mol Med (Berl).* 2018;96(7):611-20.
  - 35 Kleme ML, Sané A, Garofalo C, Seidman E, Brochiero E, Berthiaume Y, et al. CFTR deletion confers mitochondrial dysfunction and disrupts lipid homeostasis in intestinal epithelial cells. *Nutrients.* 2018;10(7):836.
  - 36 Sacoman JL, Dagda RY, Burnham-Marusich AR, Dagda RK, Berninsone PM. Mitochondrial O-GlcNAc transferase (mOGT) regulates mitochondrial structure, function, and survival in HeLa cells. *J Biol Chem.* 2017;292(11):4499-518.

Received May 10, 2020

Accepted after revision September 16, 2020